ORIGINAL PAPER

Convenient formation of nanoparticle aggregates on microfluidic chips for highly sensitive SERS detection of biomolecules

**Jianhua Zhou · Kangning Ren · Yihua Zhao ·
Wen Dai · Hongkai Wu**

Abstract Microfluidic chips combined with surface-enhanced Raman spectroscopy (SERS) offer an outstanding platform for rapid and high-sensitivity chemical analysis. However, it is nontrivial to conveniently form nanoparticle aggregates (as SERS-active spots for SERS detection) in microchannels in a well-controlled manner. Here, we present a rapid, highly sensitive and label-free analytical technique for determining bovine serum albumin (BSA) on a poly(dimethylsiloxane) (PDMS) microfluidic chip using SERS. A modified PDMS pneumatic valve and nanopost arrays at the bottom of the fluidic microchannel are used for reversibly trapping gold nanoparticles to form gold aggregates, creating SERS-active spots for Raman detection. We fabricated a chip that consisted of a T-shaped fluidic channel and two modified pneumatic valves, which was suitable for fast loading of samples. Quantitative analysis of BSA is demonstrated with the measured peak intensity at $1,615~cm^{-1}$ in the surface-enhanced Raman spectra. With our microfluidic chip, the detection limit of Raman can reach as low as the picomolar level, comparable to that of normal mass spectrometry.

Keywords Microfluidics · Gold nanoparticles · Aggregates · Surface-enhanced Raman spectroscopy · Highly sensitive detection

J. Zhou · K. Ren · Y. Zhao · W. Dai · H. Wu (✉)
Department of Chemistry,
The Hong Kong University of Science and Technology,
Clear Water Bay, Kowloon, Hong Kong, China
e-mail: chhkwu@ust.hk

Introduction

Microfluidics offers an excellent platform for analytical and biomedical testing, because of its many advantages such as low consumption of chemicals, short time of analysis, portability for point-of-care detection, and easy integration with electronics [1–4]. At present, although many efforts have been made for rapid and high-sensitivity detections on chip, the analyses are compromised by the extremely small detection volume available for measurements [5–8]. Among all optical methods, fluorescence, especially laser-induced fluorescence, has been most widely used for on-chip detection mainly because of its high sensitivity as well as its relatively easy integration with microchips [9]. Nevertheless, many chemical and biological species do not fluoresce and have to be labeled with fluorescent tags to allow fluorescence detection. In contrast, Raman spectroscopy provides a label-free analytical method that can give a fingerprint spectrum of the analyte molecule by probing the vibrational states of the molecule [10, 11]. With this technique, it is possible to identify non-fluorescent molecules as well as to simultaneously detect multiple analytes because the peaks in the spectrum are relatively narrow. However, the major challenge for normal Raman spectroscopy is that the signal of scattered light is very weak therefore limits its sensitivity. In the past decades, surface-enhanced Raman spectroscopy (SERS) has been demonstrated to be powerful for amplifying molecular Raman scattering signals based on adsorption to metal nanostructures [12–15]. The strong enhancement of SERS signals originates from the electromagnetic field-enhancement effect at so-called SERS-active "hot spots," which are normally rough metal surfaces or metal nanostructures (e.g., silver or gold). In particular, large field enhancement can be obtained at the location where particles are closely in touch with each other, e.g. in

nanoparticle aggregates. The typical enhancement factors of SERS are ~10^6–10^{10}, and it has been reported that SERS can achieve single molecule level detection [16, 17].

In nanoparticle-based SERS techniques, because SERS signals drop rapidly with increasing distance between nanoparticles, both the formation of nanoparticle aggregates and the introduction of analyte molecules to the hot spots play important roles. [18] While the common salt/analyte-driven method is not easy to control [19], microfluidics provides a convenient strategy for controlling the formation of nanoparticle aggregates. For example, Banerjee and co-workers demonstrated an interesting method for "free-surface microfluidic control" of gold nanoparticles on a microchip for continuous analysis of airborne molecules [20]. However, this approach is not amenable for molecules in aqueous solutions. Lee et al. used oxygen gas etching to create a rough polysilicon surface on a quartz wafer where gold nanoparticles were deposited for SERS measurement [21]; Kim et al. electrolessly plated gold onto poly(methyl methacrylate) microbeads and used the microbeads as SERS substrate for on-chip detection [22]. These methods require multiple steps and, similar to the continuous-flow-based SERS methods [23–25], large amount of gold for the preparation of the SERS substrates. Käll and co-workers applied optical tweezers to form aggregates of nanoparticles for SERS analysis in a microfluidic device [26]. But the requirement of sophisticated equipment in this method hinders its wide applications in research laboratories. Recently, Coté and co-workers developed a more general method for trapping nanoparticles and forming their aggregates with a nanochannel section on a microfluidic chip; they successfully applied their device for SERS study of the conformational transition of β-amyloid peptide [27–29]. However, these silicon-based nanochannels-containing microchips are very difficult to make and each chip is likely to be used for one time only.

Here, we describe a simple, low-cost poly(dimethylsiloxane) (PDMS) microfluidic chip for rapid and high-sensitivity analysis of biomolecules using Raman spectroscopy. The region of this chip for forming gold nanoparticle aggregates as SERS-active spots contains a pneumatic valve and nano-posts at the bottom surface of the microfluidic channel. When the PDMS membrane of the valve is pressed against the nanoposts, gold nanoparticles (~250 nm) are trapped in front of the valve in the microchannel, creating SERS-active sites for SERS measurements (Fig. 1). This chip is applied for on-chip analysis of trace amount of proteins (e.g., bovine serum albumin) and other biomolecules (e.g., oligonucleotide) in aqueous solutions. Compared with other methods, our approach can form nanoparticle aggregates more conveniently, and the aggregates can be released and renewed for multiple detections.
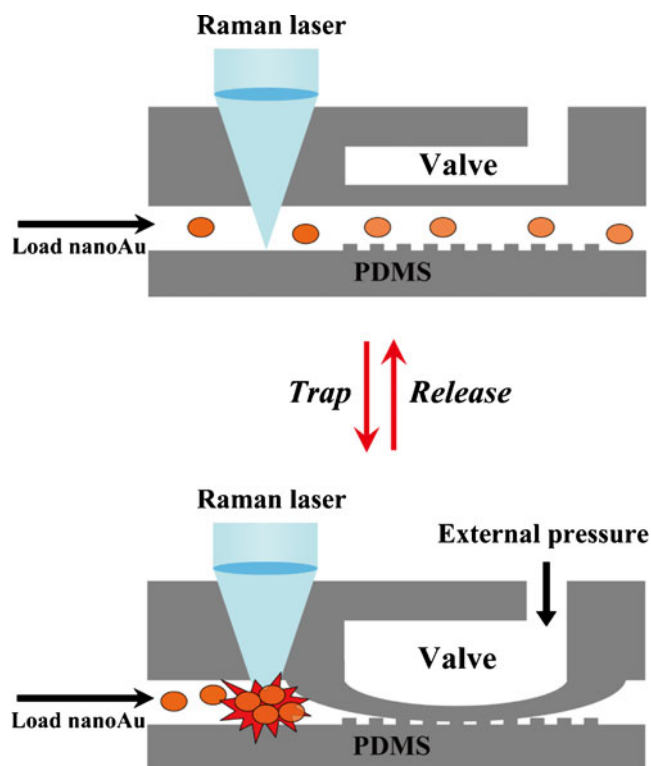
Fig. 1 Schematics of trapping and releasing of gold nanoparticles using a modified pneumatic microvalve for SERS detection

Experimental section

Materials PDMS prepolymer (components A and B, RTV 615, GE Silicones, USA), gold nanoparticles solution (0.01% in weight, average size is 250 nm, Ted Pella Inc., USA), bovine serum albumin-fluorescein conjugates (Invitrogen Corp., USA), bovine serum albumin (Sigma). The water used in all experiments was obtained by filtering through an ultrapure water system (NANOpure® DIamond™, Barnstead, USA).

Fabrication of PDMS microfluidic chip PDMS chips with valves were formed by multilayer soft lithography using previous reported methods with a variation [30, 31]. The top layer of the chip (layer with valve channel) was formed by casting PDMS prepolymer (RTV 615 A/B with a mass ratio of 10:1) against a valve master and curing the PDMS in an oven (70 °C, 30 min). The PDMS layer (~4 mm thick) was peeled from the master; holes were punched through the PDMS layer for connection to external pressure controllers. The middle layer of the chip (layer with fluidic channel) was formed by spin-coating (1,400 rpm, 30 s) PDMS prepolymer onto the channel master. After this, the channel layer was partly cured into a soft-gel state (70 °C, 7 min), the valve layer of PDMS was aligned and affixed to this channel layer under a stereoscope (Leica EC3, Leica Microsystems Ltd.). Another curing step (70 °C, 30 min)

was followed to bond the first two layers. This bonded PDMS layer was peeled from the channel master and holes were punched for connection to the sample reservoirs. The bottom layer of the chip (a flat PDMS with nanopost array on its surface) was formed by casting PDMS prepolymer onto a photoresist master, which was formed on a silicon wafer by photolithography. After degassing, curing at 70 °C for 15 min, the PDMS layer was peeled from the master. To form the whole chip, the bonded layer, which contained the valve channel (top layer) and fluidic channel layer (middle layer), was bonded together with the bottom layer using a thin layer of PDMS prepolymer (~1 μm by spin-coating on glass slide) as adhesive, followed by another curing step in an oven (70 °C, 1 h) to become an integral chip [32].

SERS acquisition Confocal surface-enhanced Raman measurements were performed on a Renishaw 2000 Raman microscope system. A He/Ne laser operating at 633 nm was used as the excitation source with a laser power of 10%. The slit, which is in front of the diffraction grating, is ~25 μm wide. The laser was focused onto a ca. 3-μm diameter spot on the sample surface via a long working distance 50× objective. The integration time was set to be 10 s, and the wave-number range was from 1,000 to 1,800 cm^{-1}. The Rayleigh line was removed from the collected Raman scattering using a holographic notch filter in the collection path. An additional CCD camera was fitted to an optical microscope to obtain optical images. All the Raman spectra were measured in the confocal mode.

Typical samples for SERS were prepared as follows. The gold colloid and samples solution were introduced into the chip using a syringe pump (Pico Plus, Harvard Apparatus, MA) at 5.0 and 10.0 μL/min, respectively. First, the gold colloid was transported into the channel and the gold nanoparticles were trapped at the entrance of the valve to form aggregates; after that, the samples (i.e, fluorescein isothiocyanate-labeled BSA (FITC-BSA), BSA, and Cyt c solutions) were subsequently loaded to the gold aggregate sites. The Raman laser beam was focused on the gold aggregates to acquire SERS signals. For each measurement, five spectra were collected from five gold aggregates with similar sizes and the intensities were averaged.

Results and discussions

Fabrication of a microchip with modified pneumatic valves

The microchip containing a T-shaped microchannel and two modified pneumatic valves is fabricated using multilayer soft lithography as described previously [33, 34]. We spin-coated a thin layer of PDMS prepolymer onto a master with a T-shape microchannel design as the fluidic channel (consist of photoresist), half-cured prepolymer in an oven at 70 °C for 7 min. We prepared a PDMS block containing two control valve channels using replica molding, then aligned it to the T-shape channel on the master and sealed them together. After another heating at 70 °C for 30 min, the totally solidified PDMS was peeled off and bonded with a flat PDMS with nanopost array on its surface to form the whole chip. Figure 2A shows the photograph of the chip obtained, bearing a T-shape fluidic channel and two valve control channels. The valve channels in the top layer are connected to an external pressure controller, and the fluidic channel in the middle layer is connected to the reservoirs. One of pneumatic valves is enlarged and shown as Fig. 2B. The valve channels (~40 μm high and ~200 μm wide) and fluidic channel (~20 μm high and ~100 μm wide) are cross in orthogonal direction (a crosswise arrangement); and there is a microarray of posts at the bottom of the fluidic channel. We cut the chip along the dash line in Fig. 2B, and the cross-section of this valve is shown as Fig. 2C. It shows that there is a thin elastomeric PDMS membrane (~80 μm) between the control valve channel and the fluidic channel. At the bottom of the fluidic channel, there is an array of nanoposts with a height of ~700 nm and a diameter of ~5 μm, which can be observed by atomic force microscope in Fig. 2D (also see, Fig. S1 in the Electronic supplementary material (ESM)). By making a small modification to the conventional pneumatic valve, we fabricate this special valve, which can block the gold particles while allowing fluids (e.g., buffer) going through.

Trapping and releasing gold nanoparticles using microvalve

To investigate the trapping and releasing processes of nanoparticles in the fluidic channel, a solution of 250-nm gold colloid (0.01% in weight, see, Fig. S2 in the ESM) is introduced into the microfluidic chip. The choosing of gold nanoparticle size is mainly based on the following considerations: (1) 250-nm gold nanoparticles are easier to be blocked by microvalve than the smaller ones; (2) the 250-nm gold nanoparticles are visible under microscope in dark field, and the SERS-active sites could be easily followed; (3) the intensity of the SERS increases with sizes of gold nanoparticle (from ~40 to ~250 nm) for similar shape [35]; (4) the surface plasmon resonance of 250-nm gold aggregates is from 500 to 800 nm (see, Fig. S3 in the ESM), it overlaps very well with the 633 nm He/Ne laser source of our Raman spectrometer [36].

The trapping and releasing process of gold nanoparticles is shown as Fig. 3. The open/closed states of the valve, shown as Fig. 3A, are controlled by the pressure applied to the valve channel: (a) when no pressure is applied, the PDMS membrane does not deform and the fluidic channel

Fig. 2 (**A**) Photograph of the chip; (**B**) top view, and (**C**) cross-section of the modified pneumatic valve, with nanopost array at the bottom of the fluidic channel; (**D**) 3D atomic force microscope image of the nanopost array
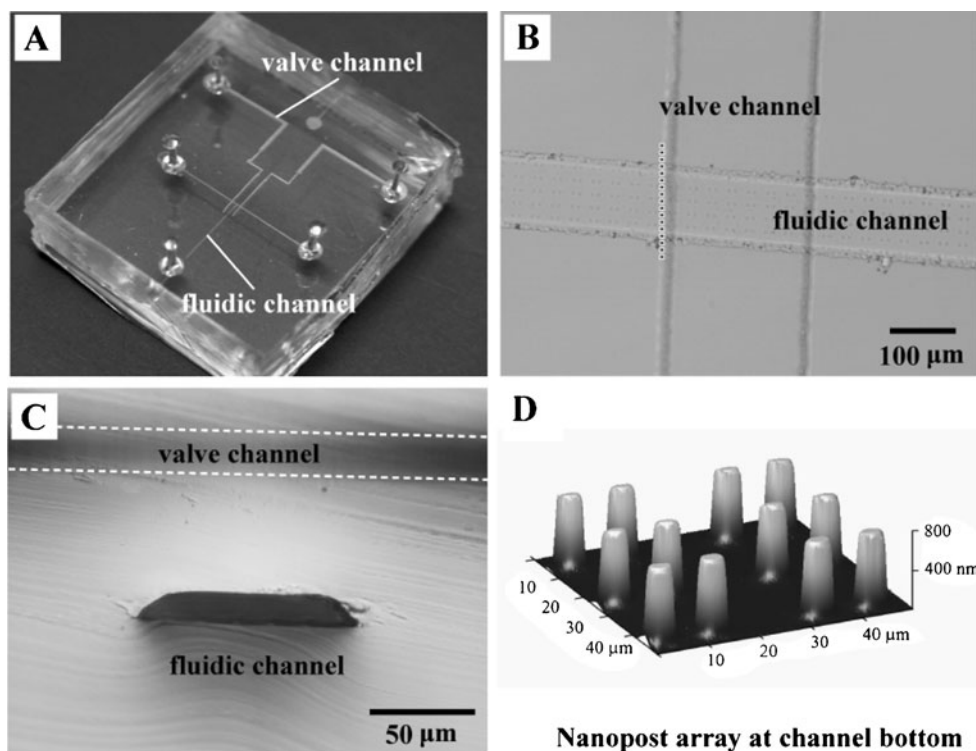

is open, therefore small particles could flow through the microvalve; (b) when a moderate pressure is applied, the membrane starts to deform and half closes the fluidic channel. Firstly, gold colloid is perfused into the channel and flows through the opened microvalve. When a moderate pressure (~20 psi) is applied to the valve channel, the thin PDMS elastomeric membrane deforms and contacts with nanoposts at the bottom of fluidic channel; the PDMS nanoposts are also forced to deform, and the degree of deformation depends on the pressure applied. Since the diameter of the gold nanoparticle is larger than the height of the deformed PDMS relief structures, the nanoparticles are trapped at the entrance of the valve and form high-density aggregates within minutes, while the buffer could still flow through the microvalve. If the pressure applied is lower than 20 psi, the valve cannot block the gold nanoparticles. Figure 3B shows schematics of the trapping and releasing process of gold nanoparticles, and Fig. 3C shows the pictures correspond to the steps of 3B. Figure 3C1 shows a bright-field image of the chip when the valve is open; Fig. 3C2 shows the image of nanoparticle aggregates (black spots) at the entrance of microvalve after loading the gold colloid for 30 min when the valve is half closed. The aggregates (within the red circle) are reproducible and easy to see under microscope. The aggregate grows with time; as shown in Fig. S4 in the ESM, more gold nanoparticles could be trapped with longer time. Therefore, large area of gold nanoparticle aggregate can be assembled at the bottom of fluidic channel, as well-defined nanostructure for SERS

detection (see, Figs. S4B (dash line rectangle) and S2 in the ESM). In order to get a reliable surface-enhanced Raman spectrum, 10~15 min is needed for complete formation of the aggregates. Comparing with Coté's method (needs ~24 h using single nanochannel), it takes less time to form the gold aggregates; the fluidic channel (at the closed state of the valve) is 100 μm wide, which is much wider than those of the reported nanochannel (5 μm wide) thus allows more aqueous solution flowing through the valve and blocking more gold nanoparticles during the same period. Also, the renewable property of gold nanoparticle aggregates is investigated. After SERS measurement of analytes on gold aggregates, we open the microvalve and wash off the gold aggregate by flushing buffer in the fluidic channel for a while. As shown in the images in Fig. 3C (steps 2 and 3), the black spots (e.g., gold aggregates) at the entrance of microvalve can be completely removed. Using this kind of microvalve, gold nanoparticles can be conveniently trapped and aggregated at the entrance of the microvalve to form SERS-active sites for confocal micro-Raman detection, and the aggregation can also be removed for successive measurement.

Chip design and operation process for rapid detection of sample

In some previous reports, the chip consists only one straight fluidic channel [27–29]; after trapping gold nanoparticles, it takes a long time and requires very high pressure to

Fig. 3 Trapping and releasing 250-nm gold nanoparticles by closing/opening microvalve. (**A**) Schematic image showing the closed/open states of the modified microvalve; (**B**) schematics showing the trapping and releasing process of gold nanoparticles. (**C**) Pictures that correspond to the steps of (**B**). The *circled numbers* show the order of the pictures, and each picture corresponds to the schematics in (**B**) with the same number. The *scale bars* are 100 μm
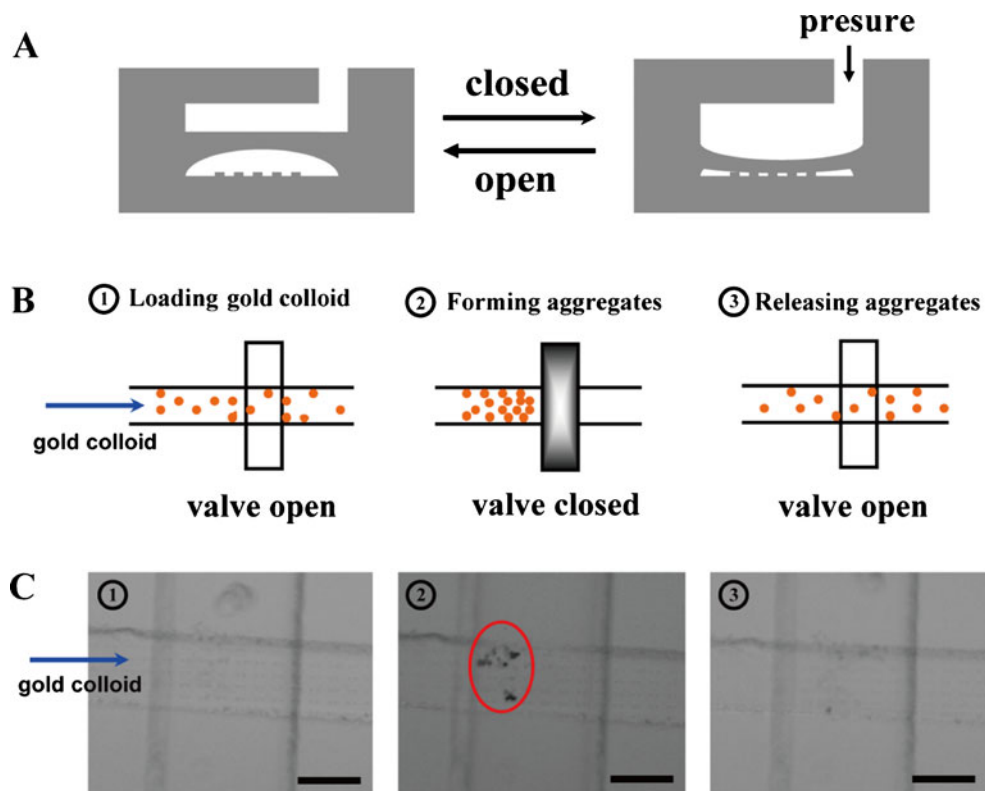
afterward load the sample solution into the same channel, by squeezing the solution going through the nanochannel. If the analytes and gold nanoparticles are pre-mixed together before loading into the chip, precipitation could form in most cases due to the adsorption of analytes onto gold particles; therefore, the gold colloid and the sample need to be introduced to the chip separately (gold colloid first, and then the sample); and the loading of sample solution costs a lot of time. To overcome this problem, we fabricate a microfluidic chip with a T-shaped fluidic channel and two valves for fast loading of samples (Fig. 4). Figure 4A schematically illustrates the process of trapping gold nanoparticles, analyzing biomolecules, and releasing both of them. The corresponding optical and fluorescence images are shown in a series as Fig. 4B.

Three steps are involved in the process of rapid detection of protein (we use fluorescein isothiocyanate-labelled bovine serum albumin, FITC-BSA, as a sample for demonstration). First, the gold colloid is introduced into the T-shaped channel. Valve 1 is half closed under a moderate pressure (~20 psi) and valve 2 is fully closed under a higher pressure (~40 psi); then the solution can only flow through valve 1. Because the height of the half-closed valve 1 is smaller than the sizes of gold nano-particles, the gold particles are trapped at the entrance of the valve 1. Although higher pressure is applied to valve 2, it still cannot totally deform the PDMS relief structures at the bottom of channel; so a little solution can also flow out

through valve 2, leading to some gold aggregates at the entrance of valve 2 as well. It does not affect our experiment because we only use the gold aggregates in front of valve 1 for detection. Subsequently, valve 2 is opened and the FITC-BSA aqueous solution is introduced into the main channel; the FITC-BSA diffuses to gold aggregate sites at the entrance of valve 1 (left valve), which takes about 3 min. Then the surface-enhanced Raman spectra of FITC-BSA are attained by focusing the laser beam at the gold aggregate sites under a confocal micro-Raman spectrometer. Using this method, the time for sample injection is significantly shortened comparing to that with the single-valve channel design. Finally, two valves are fully opened to wash off both the gold nanoparticles and analyte (i.e., FITC-BSA). Consequently, the microfluidic chip is renewed for next experimental run. A typical experiment requires only 30 min, which is much faster than that of Coté's (at least 24 h) [27]. The detection is rapid because of the less time for forming gold aggregates and fast loading of sample.

Detecting trace protein on gold aggregates using SERS on chip

To evaluate the capability of this chip for chemical analysis, a low concentration of BSA solution (0.5 nM) is measured on-chip using a confocal micro-Raman spectrometer. As shown in the inset of Fig. 5, the gold aggregates are clearly

Fig. 4 Operation process of the SERS detection on chip. (**A**) Schematics of the three states of the microvalve. (**B**) Images of the three states: (*I*) dark-field image of valve after many gold particles are trapped; (*II*) fluo-rescence image showing the diffusion of FITC-BSA to the left-side site (where gold nano-particles aggregate); (*III*) fluo-rescence image showing that FITC-BSA and gold nanopar-ticles have been washed off. The *scale bars* are 100 μm
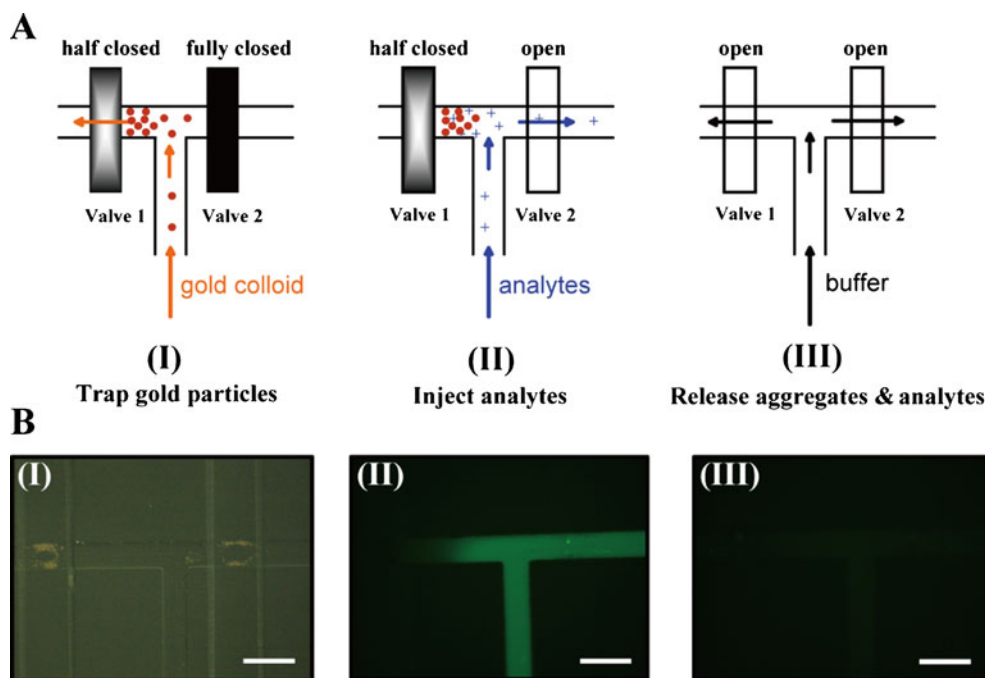
visible under a 50× microscope objective. Due to the surface plasmon of gold nanoparticles, the gold aggregates shine in dark-field image, indicating strong scattering occurs once the gold nanoparticles are aggregated, which allows us to study the performance of SERS on aggregates. The excitation laser is focused on the gold aggregates at the microvalve entrance to obtain the surface-enhanced Raman spectra of BSA molecules. As shown in Fig. 5, curve (a) shows the Raman spectrum at the gold aggregate sites before the 0.5 nM BSA (in pH 7.4 PBS buffer) is introduced. The peaks at ~1,263 and 1,413 cm^{-1} are from the asymmetric/symmetric deformation of –CH$_3$ of PDMS [37]. Although the focal depth of the laser beam is narrow, the Raman signal from a small volume of chemicals in the microchannel could not be completely separated from the signals originating from the surrounding PDMS material. Curve (b) shows the Raman spectrum from the gold aggregate sites after infusing the BSA solution. Compared with curve (a), a strong peak at ~1,615 cm^{-1} appears in curve (b), along with other peaks at ~1,145, 1,351, and 1,650 cm^{-1} which are from the Tyr, Trp or Phe, and amide I band of BSA, respectively [38, 39]. In comparison, while the laser beam is focused on the area without gold nanoparticle aggregates, curve (c) is obtained, showing no characteristic peaks of BSA. These results indicate that trace protein could be detected using the gold aggregates by surface enhancement effect, while the same concentration of BSA is undetectable in solution. Because the Raman peaks are much narrower than fluorescence bands, BSA can be detected in the presence of PDMS, suggesting that SERS

can be used for multi-analytes detection. After all measurements, gold nanoparticles and BSA are both washed away by buffer, and the peaks which are characteristics of BSA disappear in the curve (d). We perform this detection on the same chip for three times, and the reproducibility of the spectra is shown in Fig. S5 in the ESM, with a relative standard deviation of ~17% in the concentration of BSA. It
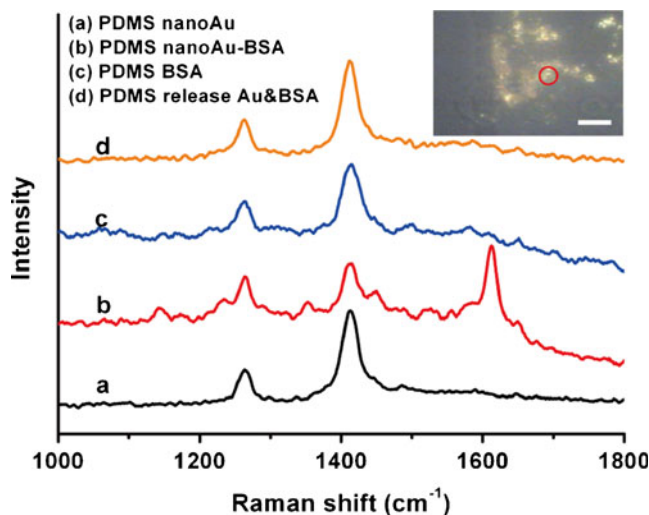
Fig. 5 Surface-enhanced Raman spectra from gold aggregates on chip with 633 nm excitation. (*a*) before loading 0.5 nM BSA solution, (*b*) after loading BSA for 15 min, focusing on gold aggregate, (*c*) after loading BSA for 15 min, not focusing on gold aggregate, and (*d*) after washing off both gold nanoparticles and BSA. *Inset*, dark-field image of gold aggregates in microchannel; the *red circle* indicates the site of laser spot, and the *scale bar* is 20 μm

further suggests that the gold aggregates could be renewed, thus the microfluidic chip is reusable.

SERS also offers a promising way for quantitative detection as demonstrated in many reports [40–44]. Although the reproducibility of surface-enhanced Raman spectrum may be a problem, it could be improved by utilizing the exact same nanoparticles for SERS or by focusing the laser on large area of assembled gold nanoparticles (area of red dash line box in Fig. S4 in the ESM) and averaging the intensities from many times of measurements. Analytes suitable for quantitative SERS experiments are those whose band lies in a region free from other interfering features (the 1,615 cm^{-1} band in this case). Also, it is convenient to have an appropriate internal standard, which can be used to compensate the changes in experimental parameters, such as fluctuations in laser power or focus onto the substrate [41]. For this work, PDMS is chosen as the internal standard, since it is inert and has a very simple Raman spectrum whose bands do not interfere with those of the BSA. Figure 6A shows a series of surface-enhanced Raman spectra with increasing concentrations of BSA. The spectra are collected from the same chip with newly-formed gold aggregates at each batch, and normalized to the peak (at 1,413 cm^{-1}) intensity of internal standard. The relative intensities of the bands at ~1,145, 1,351, ~1,580, and 1,615 cm^{-1}, which are from the BSA, increase with increasing concentration of BSA. Even at the lowest BSA concentration (100 pM), there is clearly a small band at 1,615 cm^{-1}. The heights of the peak at ca. 1,615 cm^{-1} (as I_{1615} from BSA) and the peak at ca. 1,413 cm^{-1} (as I_{1413} from PDMS) are measured. A plot of I_{1615}/I_{1413} against the concentration of BSA is linear over the range of 0~1 nM BSA with a correlation coefficient (R) of 0.996 (shown in Fig. 6B). The detection limit of SERS, on this microfluidic chip, is found to be down to the picomolar level, and this low detection limit is comparable with the result of the mass spectrometry method [43]. The low detection limit is due to the high enhancement of Raman signal, and the pre-concentration of analyte on the surface of gold nanoparticles. First, in order to obtain high SERS signals, the wavelength of the laser source of Raman spectrometer should overlap very well with the surface plasmon resonance of gold aggregates (the surface plasmon resonance of gold aggregates is related to their sizes). Second, prior to making these measurements, the analyte solution is flowed over the nanoparticles for 15 min. During this period, BSA adsorbs and accumulates on the nanoparticles for pre-concentration prior to analysis. We found that the Raman intensity became stable (reach a plateau) after 15 min, which is consistent with previous reports on the kinetics studies of BSA binding to gold nanoparticles [45]. In this system, the Raman spectroscope is applied to simultaneously detect multiple analytes on unmodified gold
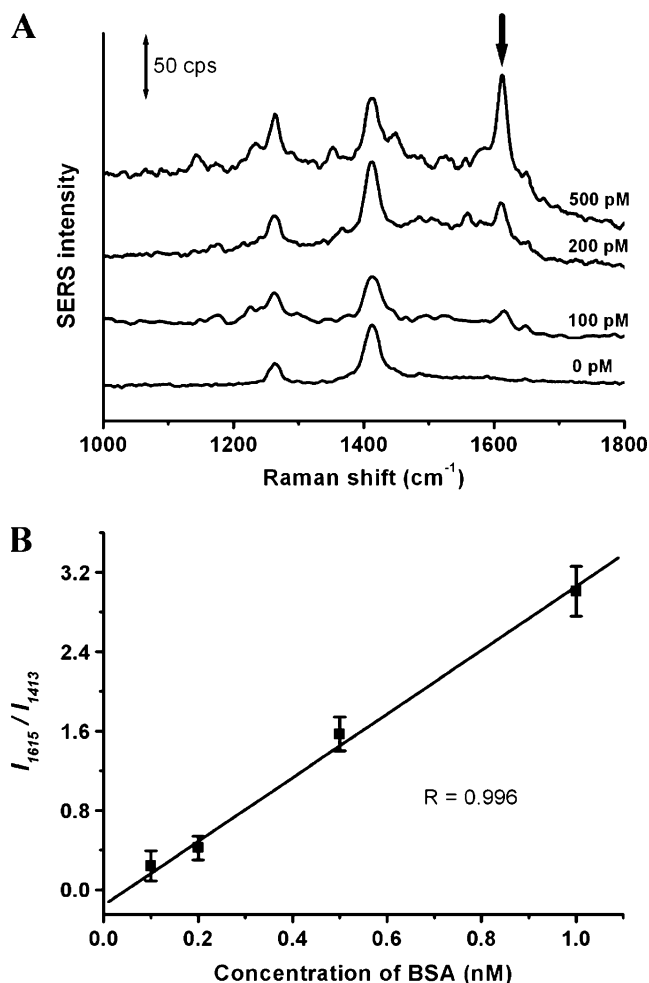
Fig. 6 (A) Surface-enhanced Raman spectra of BSA with increasing concentrations in the microfluidic channel: (*a*) 0, (*b*) 100, (*c*) 200, and (*d*) 500 pM. (B) The calibration plot obtained from the spectra of BSA with different concentrations

nanoparticles. Any analyte that is close enough to the surface of gold nanoparticles shows its spectrum with characteristic peaks [21]. Each peak in a Raman spectrum is relatively narrow so that the peaks from multiple analytes can be distinguished from each other, achieving acceptable selectivity. For example, Cytochrome c (Cyt c) can be distinguished from BSA in the BSA and Cyt c mixture (see, Fig. S6 in the ESM). By this means, it could be possible to make quantitative SERS measurements of multiple analytes. Others have successfully demonstrated it in analyzing mixtures [46]; however, it should be noted that quantification of multiple analytes can be difficult because of the complicated competition among different analytes for absorbing onto the substrate [40]. Furthermore, the selectivity of this detection method can be improved by surface modification of gold nanoparticles, such as modifying the gold nanoparticles with specific antibody to detect the corresponding antigen in the sample.

Conclusions

We have demonstrated a general PDMS microfluidic chip for conveniently trapping nanoparticles for the formation of SERS-active hot spots (nanoparticle aggregates here) and applied the chip for rapid, highly sensitive and label-free detections of biomolecules in the microchannel. Compared with silicon-based devices for SERS, this PDMS chip is cheaper and easier to fabricate. Also, the chip offers construction of a regenerative metal nanoparticle-based SERS-active site for detection of many samples successively. This technique could be useful in the situations where fast identification of dangerous biological and chemical warfare agents or monitoring of trace biomolecules is needed.

References

1. Whitesides GM (2006) The origins and the future of microfluidics. Nature 442:368–373
2. Yager P, Edwards T, Fu E, Helton K, Nelson K, Tam MR, Weigl BH (2006) Microfluidic diagnostic technologies for global public health. Nature 442:412–418
3. Weibel DB, Whitesides GM (2006) Applications of microfluidics in chemical biology. Curr Opin Cell Biol 10:584–591
4. Huang B, Wu HK, Bhaya D, Grossman A, Granier S, Kobilka BK, Zare RN (2007) Counting low-copy number protiens in a single cell. Science 315:81–84
5. Rios A, Escarpa A, González MC, Crevillén AG (2006) Challenges of analytical microsystems. TrAC Trends Anal Chem 25:467–479
6. Mogensen KB, Klank H, Kutter JP (2004) Recent developments in detection for microfluidic systems. Electrophoresis 25:3498–3512
7. Schwarz MA, Hauser PC (2001) Recent developments in detection methods for microfabricated analytical devices. Lab Chip 1:1–6
8. Viskari PJ, Landers JP (2006) Unconventional detection methods for microfluidic devices. Electrophoresis 27:1797–1810
9. Dittrich PS, Manz A (2005) Single-molecule fluorescence detection in microfluidic channels—the Holy Grail in μTAS? Anal Bioanal Chem 382:1771–1782
10. Haynes CL, Yonzon CR, Zhang XY, Van Duyne RP (2005) Surface-enhanced Raman sensors: early history and the development of sensors for quantitative biowarfare agent and glucose detection. J Raman Spectrosc 36:471–484
11. Faulds K, Littleford RE, Graham D, Dent G, Smith WE (2004) Comparison of surface-enhanced resonance Raman scattering from unaggregated and aggregated nanoparticles. Anal Chem 76:592–598
12. Hering K, Cialla D, Ackermann K, Dörfer T, Möller R, Schneidewind H, Mattheis R, Fritzsche W, Rösch P, Popp J (2008) SERS: a versatile tool in chemical and biochemical diagnostics. Anal Bioanal Chem 390:113–124
13. Popp J, Mayerhöfer T (2009) Surface-enhanced Raman spectroscopy. Anal Bioanal Chem 394:1717–1718
14. Porter MD, Lipert RJ, Siperko LM, Wang GF, Narayanan R (2008) SERS as a bioassay platform: fundamentals, design, and applications. Chem Soc Rev 37:1001–1011
15. Moskovits M (1985) Surface-enhanced spectroscopy. Rev Mod Phys 57:783–828
16. Nie SM, Emory SR (1997) Probing single molecules and single nanoparticles by surface-enhanced Raman scattering. Science 275:1102–1106
17. Xu HX, Bjerneld EJ, Käll M, Börjesson L (1999) Spectroscopy of single hemoglobin molecules by surface enhanced Raman scattering. Phys Rev Lett 83:4357–4360
18. Schwartzberg AM, Grant CD, Wolcott A, Talley CE, Huser TR, Bogomolni R, Zhang JZ (2004) Unique gold nanoparticle aggregates as a highly active surface-enhanced Raman scattering substrate. J Phys Chem B 108:19191–19197
19. Han XG, Goebl J, Lu ZD, Yin YD (2011) Role of salt in the spontaneous assembly of charged gold nanoparticles in ethanol. Langmuir 27:5282–5289
20. Piorek BD, Lee SJ, Santiago JG, Moskovits M, Banerjee S, Meinha CD (2007) Free-surface microfluidic control of surface-enhanced Raman spectroscopy for the optimized detection of airborne molecules. Proc Natl Acad Sci USA 104:18898–18901
21. Cho H, Lee B, Liu GL, Agarwal A, Lee LP (2009) Label-free and highly sensitive biomolecular detection using SERS and electrokinetic preconcentration. Lab Chip 9:3360–3363
22. Lee S, Joo S, Park S, Kim S, Kim HC, Chung TD (2010) SERS decoding of micro gold shells moving in microfluidic systems. Electrophoresis 31:1623–1629
23. Cabalín LM, Rupérez A, Laserna JJ (1996) Flow-injection analysis and liquid chromatography: surface-enhanced Raman spectrometry detection by using a windowless flow cell. Anal Chim Acta 318:203–210
24. Park T, Lee S, Seong GH, Choo J, Lee EK, Kim YS, Ji WH, Hwang SY, Gweond D, Lee S (2005) Highly sensitive signal detection of duplex dye-labelled DNA oligonucleotides in a PDMS microfluidic chip: confocal surface-enhanced Raman spectroscopic study. Lab Chip 5:437–442
25. Ackermann KR, Henkel T, Popp J (2007) Quantitative online detection of low-concentrated drugs via a SERS microfluidic system. Chem Phys Chem 8:2665–2670
26. Tong LM, Righini M, Gonzalez MU, Quidant R, Käll M (2009) Optical aggregation of metal nanoparticles in a microfluidic channel for surface-enhanced Raman scattering analysis. Lab Chip 9:193–195
27. Wang M, Jing N, Chou IH, Coté GL, Kameoka J (2007) An optofluidic device for surface enhanced Raman spectroscopy. Lab Chip 7:630–632
28. Chou IH, Benford M, Beier HT, Coté GL, Wang M, Jing N, Kameoka J, Good TA (2008) Nanofluidic biosensing for β-amyloid detection using surface enhanced Raman spectroscopy. Nano Lett 8:1729–1735
29. Wang M, Benford M, Jing N, Coté G, Kameoka J (2009) Optofluidic device for ultra-sensitive detection of proteins using surface-enhanced Raman spectroscopy. Microfluid Nanofluid 6:411–417
30. Zhou JH, Yan H, Zheng YZ, Wu HK (2009) Highly fluorescent poly(dimethylsiloxane) for on-chip temperature measurements. Adv Funct Mater 19:324–329
31. Dai W, Zheng YZ, Luo KQ, Wu HK (2010) A prototypic microfluidic platform generating stepwise concentration gradients for real-time study of cell apoptosis. Biomicrofluidics 4:024101–024114
32. Wu HK, Huang B, Zare RN (2005) Construction of microfluidic chips using polydimethylsiloxane for adhesive bonding. Lab Chip 5:1393–1398

33. Unger MA, Chou HP, Thorsen T, Scherer A, Quake SR (2000) Monolithic microfabricated valves and pumps by multilayer soft lithography. Science 288:113–116

34. Zheng YZ, Dai W, Wu HK (2009) A screw-actuated pneumatic valve for portable, disposable microfluidics. Lab Chip 9:469–472

35. Zhang Q, Li WY, Moran C, Zeng J, Chen JY, Wen LP, Xia Y (2010) Seed-mediated synthesis of Ag nanocubes with controllable edge lengths in the range of 30–200 nm and comparison of their optical properties. J Am Chem Soc 132:11372–11378

36. Westcott SL, Oldenburg SJ, Lee TR, Halas NJ (1999) Construction of simple gold nanoparticle aggregates with controlled Plasmon–plasmon interactions. Chem Phys Lett 300:651–653

37. Bae SC, Lee H, Lin ZQ, Granick S (2005) Chemical imaging in a surface forces apparatus: confocal Raman spectroscopy of confined poly(dimethylsiloxane). Langmuir 21:5685–5688

38. Han XX, Zhao B, Ozaki Y (2009) Surface-enhanced Raman scattering for protein detection. Anal Bioanal Chem 394:1719–1727

39. Zhou DF, Ke WZ, Hang H, Kang JI (2006) Raman spectroscopic study on the influence of UV radiation on BSA. J Light Scatter 18:241–247

40. Bell SEJ, Sirimuthu NMS (2008) Quantitative surface-enhanced Raman spectroscopy. Chem Soc Rev 37:1012–1024

41. Bell SEJ, Mackle JN, Sirimuthu NMS (2005) Quantitative surface-enhanced Raman spectroscopy of dipicolinic acid-towards rapid anthrax endospore detection. Analyst 130:545–549

42. Choi I, Huh YS, Erickson D (2011) Size-selective concentration and label-free characterization of protein aggregates using a Raman active nanofluidic device. Lab Chip 11:632–638

43. Lee S, Choi J, Chen LX, Park B, Kyong JB, Seong GH, Choo J, Lee Y, Shin KH, Lee EK, Joo SW, Lee KH (2007) Fast and sensitive trace analysis of malachite green using a surface-enhanced Raman microfluidic sensor. Anal Chim Acta 590:139–144

44. Mulvihill M, Tao A, Benjauthrit K, Arnold J, Yang PD (2008) Surface-enhanced Raman spectroscopy for trace arsenic detection in contaminated water. Angew Chem Int Ed 47:6456–6460

45. Brewer SH, Glomm WR, Johnson MC, Knag MK, Franzen S (2005) Probing BSA binding to citrate-coated gold nanoparticles and surfaces. Langmuir 21:9303–9307

46. Faulds K, McKenzie F, Smith WE, Graham D (2007) Quantitative simultaneous multianalyte detection of DNA by dual-wavelength surface-enhanced resonance Raman scattering. Angew Chem Int Ed 46:1829–1831